

Article

Evaluation of Satellite-Derived Surface Soil Moisture Products over Agricultural Regions of Canada

Yaasiin Oozeer ¹, Christopher G. Fletcher ^{1,*} and Catherine Champagne ²

¹ Department of Geography and Environmental Management, University of Waterloo, Waterloo, ON N2L 3G1, Canada; yaasiinoozeer@gmail.com

² Agriculture and Agri-Food Canada, Ottawa, ON K1A 0C6, Canada; catherine.champagne@canada.ca

* Correspondence: chris.fletcher@uwaterloo.ca

Received: 11 April 2020; Accepted: 2 May 2020; Published: 4 May 2020



Abstract: Soil moisture is a critical indicator for climate change and agricultural drought, but its measurement is challenging due to large variability with land cover, soil type, time, space and depth. Satellite estimates of soil moisture are highly desirable and have become more widely available over the past decade. This study investigates and compares the performance of four surface soil moisture satellite datasets over Canada, namely, Soil Moisture and Ocean Salinity Level 3 (SMOS L3), versions 3.3 and 4.2 of European Space Agency Climate Change Initiative (ESA CCI) soil moisture product and a recent product called SMOS-INRA-CESBIO (SMOS-IC) that contains corrections designed to reduce several known sources of uncertainty in SMOS L3. These datasets were evaluated against in situ networks located in mostly agricultural regions of Canada for the period 2012 to 2014. Two statistical comparison methods were used, namely, metrics for mean soil moisture and median of metrics. The results suggest that, while both methods show similar comparisons for regional networks, over large networks, the median of metrics method is more representative of the overall correlation and variability and is therefore a more appropriate method for evaluating the performance of satellite products. Overall, the SMOS products have higher daily temporal correlations, but larger biases, against in situ soil moisture than the ESA CCI products, with SMOS-IC having higher correlations and smaller variability than SMOS L3. The SMOS products capture daily wetting and drying events better than the ESA CCI products, with the SMOS products capturing at least 75% of observed drying as compared to 55% for the ESA CCI products. Overall, for periods during which there are sufficient observations, both SMOS products are more suitable for agricultural applications over Canada than the ESA CCI products, even though SMOS-IC is able to capture soil moisture variability more accurately than SMOS L3.

Keywords: soil moisture; agriculture; Canada; satellite; SMOS; ESA CCI

1. Introduction

Surface soil moisture (SM) is a key component of the Earth system which can impact weather through its influence on evaporation and surface energy fluxes [1], with a lack of SM associated with drought occurrence [2] and an excess related to flooding [3,4]. Given its importance for regional-to-global hydroclimate variability and change, SM is considered as one of the 50 Essential Climate Variables (ECVs) in the Climate Change Initiative (CCI) project established by the European Space Agency (ESA) [5]. In a Canadian context, SM availability over agricultural regions has been identified as a limiting factor to agricultural yields [6]. Furthermore, the Prairie region, which accounts for more than 80% of agricultural land in Canada, is an important global food supplier [6,7], thus highlighting the need for SM measurement for applications related to agriculture in Canada.

SM is difficult to measure due to its inherent spatial and temporal heterogeneity [8], and even though there are multiple methods available to measure SM, they all have limitations. Ground-based monitoring stations provide accurate point-scale SM estimates but they usually lack the spatial coverage to capture SM conditions over larger regions and these estimates may not be representative of soil conditions even within the vicinity of these stations [9–11]. Another common approach is to use microwave remote sensing of SM, which is promising due to the almost linear relationship between the microwave radiance emitted or reflected by the surface soil portion and the soil-water mixing ratio [12]. Even though microwave remote sensing of SM can also be challenging due to reasons related to topography [13], the presence of snow and ice [12], human-induced radio frequency interference (RFI) [14] and vegetation water [15], it provides a means to overcome the spatial limitations posed by in situ observations [16,17].

The Soil Moisture and Ocean Salinity (SMOS) mission [18,19], launched by the European Space Agency (ESA) in November 2009, was the first Earth observation mission dedicated to SM mapping. The SMOS satellite uses L-band technology (1–2 GHz), which is known to minimize attenuation of microwave signals by the atmosphere and underlying vegetation [18–23] and was shown to capture SM over time in a stable and consistent pattern over Canadian agricultural regions [24,25]. However, SMOS is also known to exhibit a dry bias, especially over arid regions [25–30] and to overestimate SM after large rainfall events [25,29]. There have been attempts to improve SM retrievals from SMOS, such as the development of a gridded multi-orbit (MO) SMOS Level 3 product [31] which showed improvements in the number of successful retrievals and wetter retrievals as compared to SMOS Level 2. SMOS-INRA-CESBIO (SMOS-IC) [32] is another more recent product which was shown to correspond better to the European Centre for Medium-Range Weather Forecasts (ECMWF) SM as compared to SMOS Level 3 [32].

Combining information derived from satellite-based passive and active microwave sensors has been reported to, potentially, not only provide improved SM estimates globally but also better spatial coverage and increased number of observations [33]. This approach of blending multiple products has also been employed to improve estimates of other climate variables, such as snow water equivalent [34]. The ESA CCI (Climate Change Initiative) SM project was established to develop a long-term soil moisture product from multiple active and passive microwave sensors, in response to the need for a climate data record of satellite SM [35]. This blended active-passive product combines the strengths of each included single-sensor SM product, one of which is SMOS [35]. Given its potential to provide improved SM estimates and the need for SM measurement over Canadian agricultural regions [6], the ESA CCI product could therefore be a useful tool for agricultural applications over Canada.

While the ESA CCI product has been evaluated against ground observations over the United States, China and Europe [36–41], such studies over Canada are limited [42,43]. Furthermore, the impact of algorithmic changes to the merging of active and passive satellite products in the last major release of ESA CCI SM [44] on SM retrieval over Canada is still unknown. To date, the assessment of SMOS Level 3 products over Canada is limited to its sensitivity to freeze/thaw cycles [45], while SMOS-IC has not been evaluated to our knowledge. Therefore, the primary objective of this study is to evaluate whether the recent improvements to the SMOS and ESA CCI products have led to improved accuracy in the SM retrievals over Canada, compared to in situ observations. A secondary objective is to compare the best performing versions of SMOS and ESA CCI and determine which one is best overall for agricultural applications over Canada.

This article is organised as follows. Section 2 contains a description of the in situ networks and satellite-based products used in this study and the methods used to evaluate the datasets. We present the results of the comparison in Section 3. In Section 4, we discuss the accuracy of the individual satellite SM products and the key differences between them.

2. Data and Methods

2.1. In Situ Soil Moisture Data

The three in situ networks used to evaluate satellite-derived SM products over Canada are shown in Figure 1. The Ontario and Manitoba networks are run by Agriculture and Agri-Food Canada as part of the Real Time In Situ Monitoring for Agriculture (RISMA) network while the Alberta network, also called the Alberta Ground Drought Monitoring Network (AGDMN), is run by Alberta Agriculture and Rural Development. While all three networks are located in predominantly agricultural regions, they serve different purposes. The Ontario and Manitoba networks consist of multiple stations covering a relatively small area to capture SM variation within the radiometer footprint for validating modelled and satellite observed SM data while the Alberta network is a mesoscale network (mesonet) which captures SM variability over the province [25]. Even though the pixel-to-point comparison of SM is challenging due to the uncertainties associated with SM variability within a pixel footprint, previous studies have reported good agreement between coarse resolution satellite SM products and these networks [11,25]. Furthermore, while other physical measurement methods of SM have shown promise in addressing some of these challenges in some parts of the world [46], further research is required to assess their full potential for Canada [47]. The proportion of agricultural land, the cultivation practices, the landscape type, the soil and the climate also vary between the above network sites. A brief description of these networks is provided below.

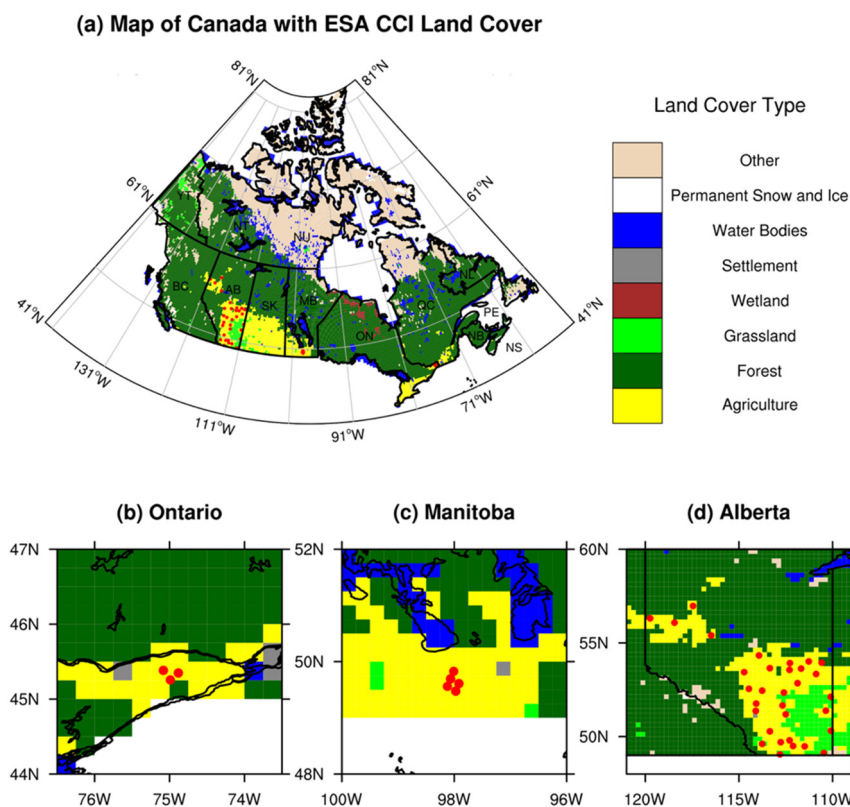


Figure 1. Location of in situ soil moisture monitoring sites in agricultural regions of Canada used in this study. (a) Map of Canada and zoomed in regions of (b) Ontario, (c) Manitoba and (d) Alberta showing the location of monitoring stations. In situ monitoring station locations are represented by red dots. Some stations are shown to overlap each other in (b) and (c) due to their close proximity. The land cover types, shown at 0.25° , are obtained from the most recent ESA CCI Land Cover map [48] and are grouped based on the IPCC land categories [48].

The stations in the RISMA network consist of three sets of replicate dielectric probes (Stevens Hydra Probe SDI-12) installed vertically at 0–5 cm and horizontally at 5 cm, 20 cm, 50 cm and, for some stations, at 100 cm. The Manitoba network consists of nine stations distributed over a largely agricultural region in the Prairie/Boreal Plain Ecozone in the Red River watershed and covers two main soil types, namely, heavy Red River clay soils to the northeast and sandier loam soils to the southwest. The Ontario network consists of five stations over largely agricultural land which covers an area of about 20 × 20 km surrounded by patches of forest and which consists mainly of cultivated corn and soybean. Stations located over clay soils were previously reported to have less SM variability and retain wetness longer than sandy soils [25] and to have representativeness issues in Manitoba [11]. Therefore, classification of soil textures derived from the RISMA Network Metadata document [49] for both networks is given in Table 1. The term representativeness above refers to the ability of in situ stations to represent SM conditions of the field in which they are located.

Table 1. Real Time In Situ Monitoring for Agriculture (RISMA) networks soil texture classification. More detailed information, such as the location of the stations within these networks, can be obtained from the RISMA Network Metadata [49] document.

Soil texture type	Ontario	Manitoba
Sand (Sand, Sand Loam, Loam)	ON2, ON5	MB1, MB4, MB7, MB9
Clay (Clay, Heavy Clay, Clay Loam, Sandy Clay Loam)	ON1, ON3, ON4	MB2, MB3, MB5, MB6, MB8

The Alberta network spans from 49°N to 56°N over the agricultural regions of the province. The northern region of the network is dominated by Boreal plain while the generally drier and warmer southeastern region is covered with mixed Prairie grasslands. Each station in the network consists of dielectric probes (Delta-T Theta) buried horizontally at 5 cm, 20 cm, 50 cm and 100 cm but none installed vertically. Data from 33 of the 38 stations are used in this work based on data availability for the duration of the study period. In addition, SM data for all networks are quality checked to remove unrealistically extreme values, and SM values below 0 m³ m⁻³ and exceeding 1 m³ m⁻³ are removed before computing the metrics for analysis. This process revealed that some stations over Alberta (such as Oyen and Oliver) recorded erroneous SM values exceeding 2 m³ m⁻³ for the year 2017 (not shown).

2.2. Satellite-Derived Soil Moisture Products

2.2.1. SMOS Products

Global SM is monitored every 3 days by the SMOS satellite, with ascending and descending overpasses occurring at 6:00 and 18:00 local time, respectively [18,19]. The SMOS SM retrieval algorithm [50], which is used to produce the SMOS Level 2 (L2) SM product, retrieves SM by minimising the squared differences between the L-Band microwave emission of the biosphere (L-MEB) [51] forward simulations of multi-angular dual-polarisation brightness temperatures (TB) and the corresponding SMOS observations. Dynamic auxiliary data such as rainfall, snow, freeze defreeze and temperature are obtained from the European Centre for Medium Range Weather Forecasts (ECMWF) forecasts. The SMOS Level 3 (L3) [31] product used here provides enhanced robustness and quality of SM retrievals as compared to L2 by using several orbits, rather than a single orbit, to account for angular sampling and radiometric accuracy at the border of the swath. However, the algorithms in both products employ the same bottom-up approach to obtain simulated TB values at the sensor resolution and are impacted by the uncertainties associated with the higher resolution auxiliary data, such as land cover maps, which are used to characterise pixel heterogeneity [32]. The daily L3 product available on a 25 km Equal-Area Scalable Earth Grid version 2.0 (EASE-Grid 2.0) is used in this study and only data for the ascending orbit are used since data for both orbits were reported to be similar for the study region [25].

The SMOS-INRA-CESBIO (IC) product [32] differs from the L3 product in the following ways. Firstly, the IC algorithm does not take into account pixel land use and assumes the pixel to be homogeneous. Thus, the IC product is independent of the ECMWF SM auxiliary data used in the L2 and L3 algorithms to estimate TB in the sub pixel fractions of heterogeneous pixels. Secondly, the L-MEB vegetation and soil parameters in the IC product were calibrated using in situ SM measurements, based on the more recent findings of Fernandez-Moran et al. [52] and Parrens et al. [53], and differ from those used in the L2 and L3 products and which were defined from literature before the launch of SMOS. Thirdly, while the L3 algorithm is based on SMOS Level 1 C TB data, which contain multi-incidence angle TB at the top of the atmosphere, the SMOS-L3 full-polarisation angle-binned TB product is used in the IC algorithm for its ease and convenience of use. Finally, in the cost function including observed and modelled TB, the SM a priori values are obtained from ECMWF reanalysis data and the SM standard deviation is set to $0.7 \text{ m}^3 \text{ m}^{-3}$ in L3 [31] while both the a priori SM and SM standard deviation are set to $0.2 \text{ m}^3 \text{ m}^{-3}$ in IC [32].

2.2.2. ESA CCI Soil Moisture

The ESA CCI SM daily product is obtained by merging Level 2 SM datasets from available active and passive microwave sensors, for which the error characteristics are known [35]. Full documentation of the ESA CCI SM product is provided by Dorigo et al. [35], and information on the merging process can be found in the Algorithm Theoretical Baseline Document (ATBD) [44]. Briefly here, passive microwave products produced with the Land Parameter Retrieval Model (LPRM) [54] and active microwave SM products generated with the TU Wien method [55,56] are included given their consistency between the different sensors [33,57,58]. The Level 2 SM retrievals from all sensors are first interpolated to a common daily time step (0:00 UTC \pm 12h) using a nearest neighbour search in time. The radiometer-based products are scaled based on the Advanced Microwave Scanning Radiometer for the Earth Observing System (AMSR-E) [54] SM using cumulative distribution function (CDF) matching [33] and merged into a radiometer-only product known as PASSIVE. The scatterometer-based products are scaled with Advanced Scatterometer (ASCAT) [59] SM moisture and merged into a scatterometer-only product (ACTIVE). Finally, the ACTIVE and PASSIVE products are scaled using SM from GLDAS-Noah v1 [60] and then merged into a COMBINED product. The merging process employs a weighted average of measurements from all available sensors at each time step using triple collocation (TC) analysis [61]. For our study period of 2012 to 2014, ESA CCI contains information from two passive satellite products, namely SMOS and AMSR2 [62], and one active product, ASCAT-A/B. However, the SMOS product included here is a LPRM-based SMOS product, which ensures consistency with other passive products blended in ESA CCI [63].

The COMBINED products versions 3.3 (CCI3) and 4.2 (CCI4), provided at a 0.25° spatial resolution, are used in this study. Furthermore, the above description of the merging process is the one employed for CCI3. CCI4 differs from CCI3 in three important ways. First, in CCI4, GLDAS-Noah soil temperature and Snow Water Equivalent estimates are used to mask out unreliable retrievals before performing CDF-Matching and TC error estimation. Second, before merging into the COMBINED product, “frozen” flags of the passive products are used to mask out unreliable retrievals in the active products and vice versa. Third, CCI4 combines all active and passive L2 products directly after CDF-Matching against GLDAS-Noah, instead of merging the pre-merged ACTIVE and PASSIVE products as in CCI3. Since the first ESA CCI product (v0.1) was released in 2012, every release has been continuously updated in the near present by introducing new satellite sensors over time [35].

2.2.3. Evaluation Strategy and Comparison Metrics

SM is evaluated for the months May to October when most land areas are snow-free over the study sites, and for the period 2012 to 2014 when ground data are consistently available from all networks. All statistical metrics are calculated for days when SM data are available for all products. In general, SMOS has more missing observations than ESA CCI, with 45% and 11% fewer days of data over the

RISMA and Alberta networks, respectively. While there is virtually no difference between the number of days of data between CCI3 and CCI4 over all regions, IC has an average of 49% fewer days of data over Ontario and Manitoba and 27% fewer over Alberta as compared to L3. This difference between the SMOS products can be attributed to the use of different input TB products. The fixed angle L3 TB used in IC includes many corrections, which eliminate TBs impacted by anthropogenic (RFIs) and spurious effects (sun impact) [31], as compared to the multi-incidence angle L1 C TB used in L3 [32].

SM measurements at 5 cm depth available from all networks are used to evaluate the satellite SM products, which are all provided in volumetric units ($\text{m}^3 \text{m}^{-3}$). For each in situ station, satellite data are extracted from the pixel that includes the point location of the station and compared with in situ measurements using several commonly-used statistical metrics, namely, the Pearson correlation coefficient (R ; Equation (1)), the bias (Bias; Equation (2)), the relative bias (Relative Bias; Equation (3)), the root-mean-square difference (RMSD; Equation (4)), the unbiased root-mean-square difference (ubRMSD; Equation (5)) and the normalized standard deviation (SDV; Equation (6)). The above metrics are calculated as follows:

$$R = \frac{\frac{1}{N} \sum_{n=1}^N (Sat_n - \overline{Sat})(InSitu_n - \overline{InSitu})}{\sigma_{Sat}\sigma_{InSitu}} \quad (1)$$

$$Bias = \frac{1}{N} \sum_{n=1}^N (Sat_n - InSitu_n), \quad (2)$$

$$Relative\ Bias = \frac{Bias}{InSitu} \times 100, \quad (3)$$

$$RMSD = \sqrt{\frac{1}{N} \sum_{n=1}^N (Sat_n - InSitu_n)^2} \quad (4)$$

$$ubRMSD = \sqrt{\frac{1}{N} \sum_{n=1}^N \{[(Sat_n - \overline{Sat}) - (InSitu_n - \overline{InSitu})]^2\}} \quad (5)$$

$$SDV = \frac{\sigma_{Sat}}{\sigma_{InSitu}} \quad (6)$$

where Sat is SM measured by the satellite, $InSitu$ is SM measured at an in situ station, N is the number of daily observations and σ_{Sat} and σ_{InSitu} are the standard deviations (computed over all days of the evaluation period) of the satellite and in situ measurements, respectively. We also assess the ability of the satellite products to capture wetting and drying by using standardized daily SM anomalies calculated with respect to the evaluation period [25,64]. We employ the nonparametric Kruskal–Wallis test [65] to identify the statistical significance of differences between the distribution of SM anomalies between the satellite and in situ products, and the Wilcoxon rank sum test [66] is used for post-hoc pairwise comparisons between the products.

Statistical comparison of SM from in situ networks and satellite products often involves arithmetically averaging SM from all stations within a network before calculating statistical metrics like SDV, R and ubRMSD (henceforth Method A) [11,25,29]. However, some studies have used an alternative approach for measurement networks that cover larger spatial domains, where the statistical metrics are calculated for each station separately and the median for each metric is selected: the so-called “median of metrics” method (henceforth Method B) [67,68]. In this study, since we compare satellite SM with in situ SM across both large and small measurement networks, both methods are used and compared. For the median of metrics method, the spatial standard deviation across all stations for each network and for each metric is also included.

3. Results

3.1. Comparison of the Satellite-Derived Products with In Situ Networks

We begin by examining the consistency in temporal variation of SM, as estimated from the absolute ($\text{m}^3 \text{m}^{-3}$) in situ measurements and the satellite products. Figure 2 shows time series of warm-season (May to October) SM for Ontario, Manitoba and Alberta from 2012 to 2014. The in situ measurements reveal a saw-tooth pattern of variability, comprising large periodic spikes associated with rainfall events, followed by multi-week periods of drying. All of the satellite products represent this observed variability fairly well, although the ESA CCI products show noticeably more daily-frequency variability, but less intraseasonal variability than in situ measurements. The SMOS products have a much larger range of intraseasonal variability than ESA CCI, leading to qualitatively worse agreement with the in situ measurements than for ESA CCI. Features such as the higher frequency of spikes associated with rainfall events in Ontario as compared to Manitoba [25], and a consistent drying trend of $>0.1 \text{ m}^3 \text{m}^{-3}$ throughout the season in Alberta, are also captured by all satellite products. Finally, all satellite products show similar mean SM to the observed SM, but with some notable biases. The average bias over Ontario, Manitoba and Alberta is generally smaller for ESA CCI (0.04, -0.05 and $-0.04 \text{ m}^3 \text{m}^{-3}$) as compared to SMOS (-0.05, -0.11 and $-0.09 \text{ m}^3 \text{m}^{-3}$).

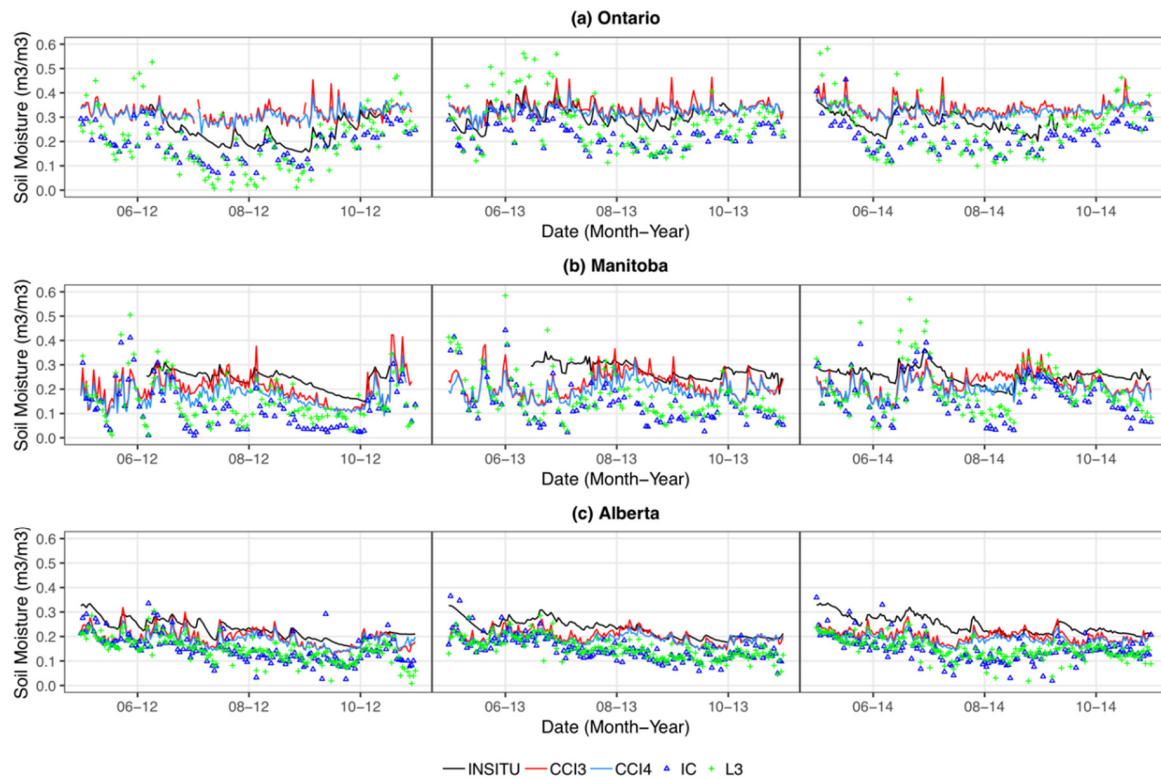


Figure 2. Time series of in situ, CCI3, CCI4, IC and L3 absolute surface soil moisture for the months May to October for a three-year evaluation period (2012–2014) at (a) Ontario, (b) Manitoba, (c) Alberta. Soil moisture data shown for each region are averages of all stations for each respective region.

In Figure 3 we compare the temporal variability and correlation between in situ and satellite SM products. While the SMOS products have larger biases in mean and variability, we find that their correlations with in situ measurements are somewhat higher than for the ESA CCI products for all networks. The average correlations over Ontario for ESA CCI and SMOS are $R = 0.6$ and $R = 0.8$, respectively, and are typically lower over Manitoba for both ESA CCI ($R = 0.5$) and SMOS ($R = 0.7$). Figure 3c also shows higher correlations ($R > 0.8$) for the SMOS products as compared to the ESA CCI products for most stations over Alberta. Furthermore, CCI4 tends to show higher correlations than

CCI3, and IC tends to show higher correlations than L3, at all networks. Figure 3 also confirms that SMOS has larger variability than in situ measurements and ESA CCI, with CCI4 generally having lower variability than CCI3 and IC having lower variability than L3, at all networks. While the variability for both ESA CCI products is typically close to that of in situ measurements, the variability for the SMOS products varies widely at the different observing networks. For instance, the variability for L3 is twice the variability of IC over Ontario, but they are much more similar over Manitoba.

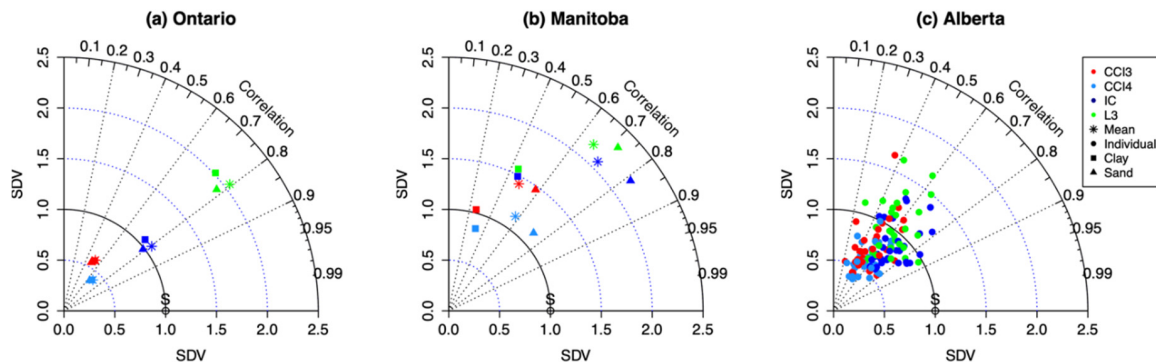


Figure 3. Taylor Diagrams [69] showing a multi-metric statistical comparison between CCI3, CCI4, IC and L3 and in situ soil moisture measurements at 5 cm depth (S) for (a) Ontario, (b) Manitoba and (c) Alberta. These diagrams show the relative position of the satellite soil moisture data to the reference in situ data using temporal linear correlation coefficient and normalized standard deviation. The closer a point is to the in situ measured value, the closer the satellite data is to the ground measured data. The Taylor diagrams for Ontario and Manitoba also include points corresponding to the mean of stations located over different soil types, that is, sand and clay.

We also perform this analysis separately for stations located in sandy and clay soils, to investigate whether soil type explains the lower correlations seen over Manitoba as compared to Ontario (Figure 3a,b). The correlations obtained for stations in Manitoba located in clay soil are systematically lower than those located in sand (Figure 3b). The correlations for Manitoba stations located in sand agree closely with the correlations for all stations over Ontario ($R \sim 0.7\text{--}0.8$ for SMOS and $R \sim 0.6\text{--}0.7$ for ESA CCI), where there is very little difference between sandy and clay locations (Figure 3a). This suggests that, for an in situ SM network containing both clay and sand stations, the in situ measurements for clay stations that have representativeness issues, such as those located over Manitoba [11], can reduce correlations of that network with satellite products. For Manitoba, we also observe that the ESA CCI products closely match in situ variability regardless of the soil type, while SMOS variability matches in situ variability more closely for clay stations, though not as well as ESA CCI, and it is at least twice as large for sand stations. In contrast, the differences in correlation and variability for different soil types are negligible for all satellite products over Ontario.

Finally, we examine whether the evaluation of satellite SM products is different for Method A versus Method B (see Section 2.2.3). Figure 4 shows that both methods produce highly similar results over the smaller Ontario and Manitoba networks: the SMOS products show higher correlations, RMSD and variability than the ESA CCI products. One advantage of Method B is that it allows quantification of spatial variability in the statistical metrics, and the righthand panels of Figure 4 reveal considerably greater spatial variability for all metrics over Manitoba as compared to Ontario. Over the large, spatially-distributed Alberta network, both methods produce similar relative biases, RMSD and ubRMSD. However, there are some notable differences in the correlation and variability between the different versions of the ESA CCI and SMOS products (Figure 4a,b,i,j). For example, Method A shows that L3 has larger correlation and smaller variability than IC, while Method B shows the reverse, which is in closer agreement to the overall performance over Alberta (Figure 3c). We find higher correlations in IC than L3 at 84% of the stations, and smaller variability at all stations (not shown).

This suggests that Method B is more appropriate to assess the correlation and variability over a spatially-distributed network like the one in Alberta.

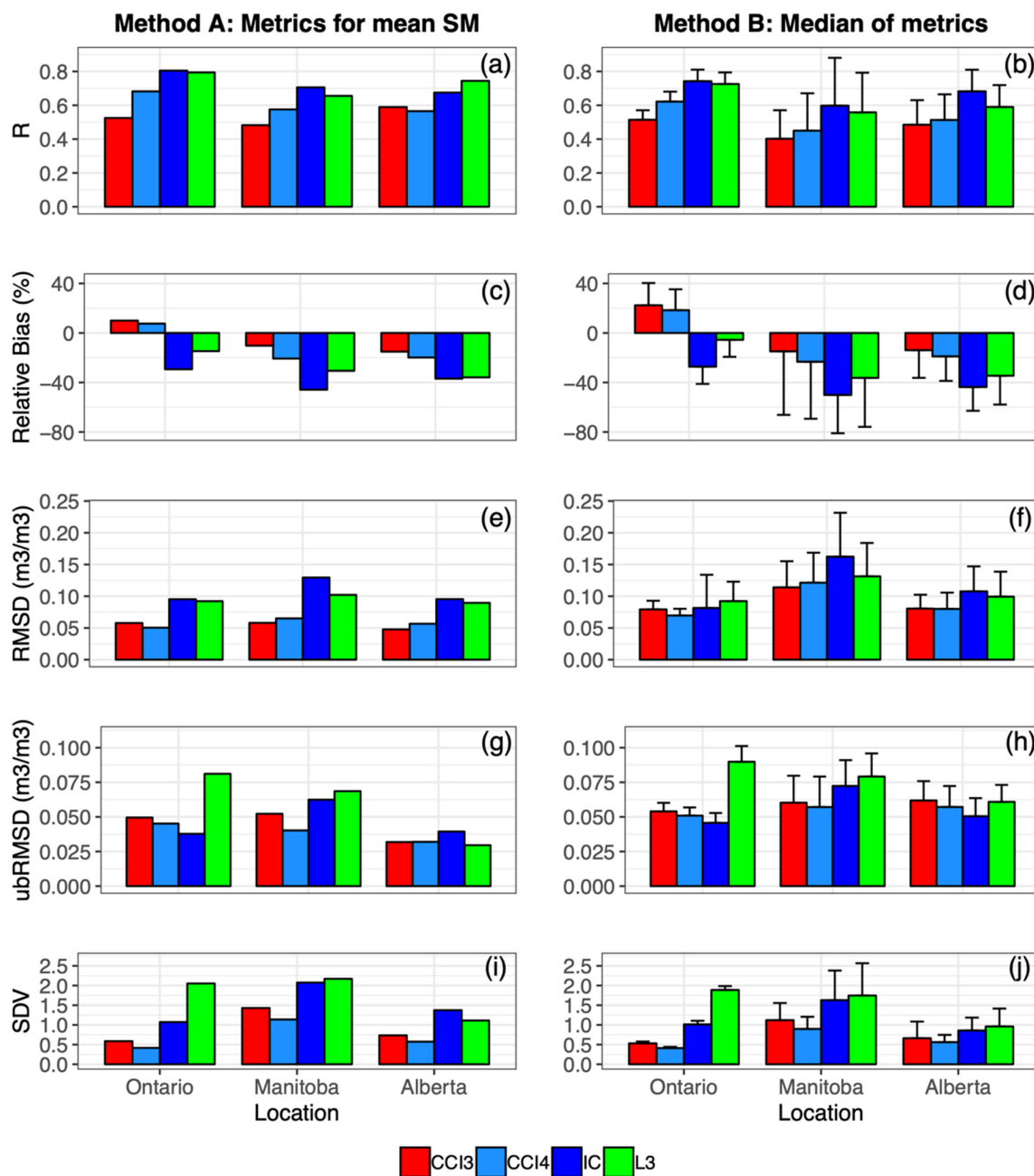


Figure 4. SM evaluation metrics – (a–b) R, (c–d) Relative Bias, (e–f) RMSD, (g–h) ubRMSD and (i–j) SDV – for the Ontario, Manitoba and Alberta networks for the period 2012 to 2014. The two methods used for statistical comparison are the method A: metrics for mean SM calculated from all stations in each network (**left column**) and method B: the median of metrics for individual stations in a network (**right column**). The error bars for the median of metrics plots represent the standard deviation across the stations in each network.

3.2. Capturing Wetting and Drying Events over Agricultural Landscapes Using Satellite-Based SM

Since agricultural applications are mostly affected by periods of anomalously high/low SM, in this section we evaluate the ability of the different satellite products to capture the statistical distribution of *standardized anomalies* of daily SM (SM') binned by the sign of the in situ anomaly for each day. Figure 5a

shows the distribution of in situ anomalies for wetting ($SM' > 0$) is skewed toward extreme wet days, with 75% of values below 1 s.d. in Ontario and Manitoba and individual extreme wet days as large as 4 or 5 s.d. Alberta SM' tends to be the most variable for wetting, with only 50% of the days below 1 s.d.. The in situ measurements for drying ($SM' < 0$) reveal almost the opposite behavior, skewed toward dry extremes but with fewer large outlier days than for the wetting events, with Ontario and Manitoba slightly more variable than Alberta (Figure 5b). We suspect that this behaviour for Alberta is due to the larger apparent SM variability during the wetter first half of the warm season every year as compared to SM variability during the drier second half (Figure 2), while for Ontario and Manitoba, there seems to be larger variability in the local minimums throughout the warm season during the study period.

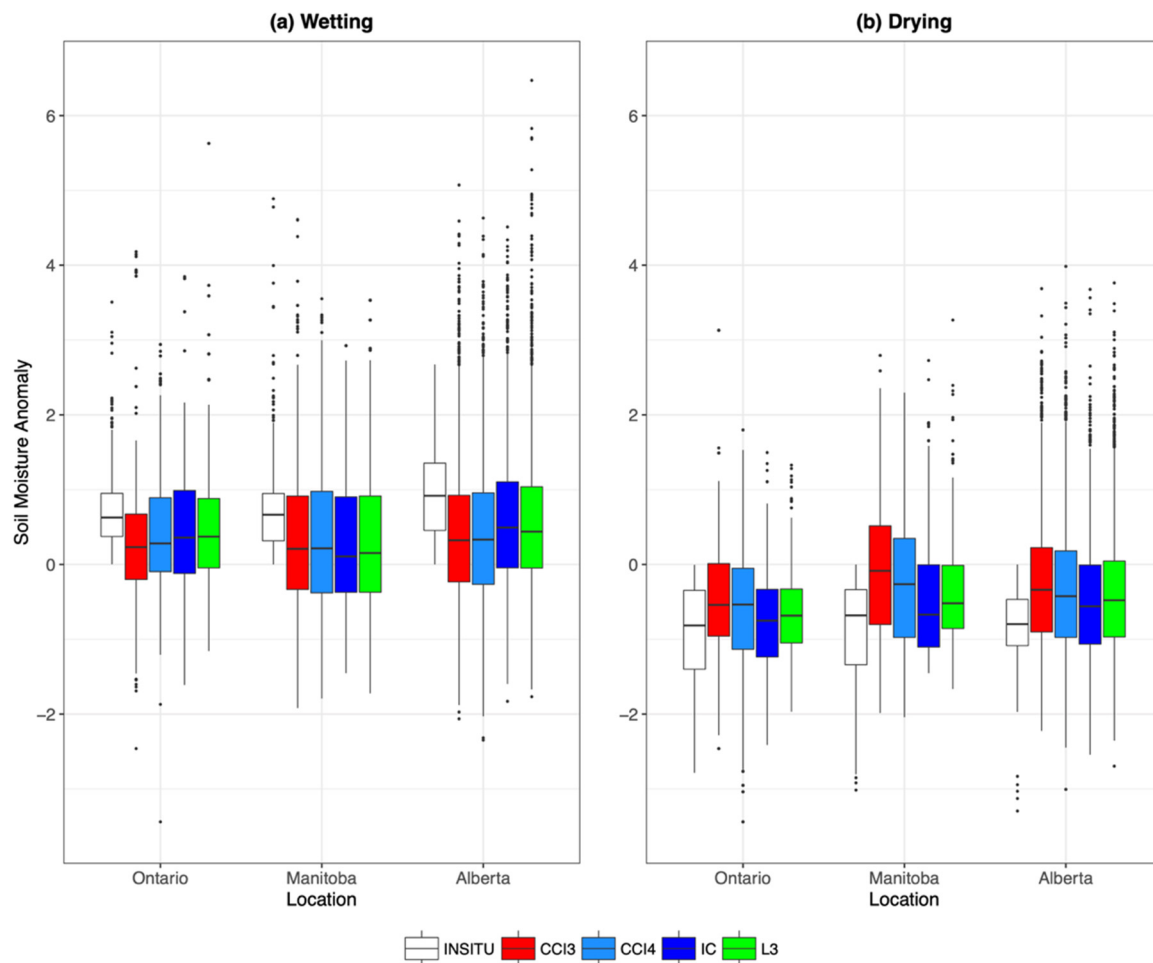


Figure 5. Boxplots of standardized SM anomalies for in situ, CCI3, CCI4, IC and L3 over May to October for a three-year evaluation period (2012–2014) at Ontario, Manitoba and Alberta networks. The figure shows SM anomalies for each satellite product binned by the sign of the in situ anomaly: (a) positive (wetting) and (b) negative (drying). For each network, the boxplots are constructed from a pool of all daily SM anomalies for all stations within that network, for only those days when data are available for all products at a given in situ location.

Turning to the satellite products, the mean anomaly across all networks and all satellite products is closer to zero than the in situ mean for both wetting and drying, due to a substantial number of days where the sign of the anomaly is opposite to the in situ data. For wetting, the large number of negative values for all products—representing drying during periods when in situ is wet—indicates considerable disagreement in post-rainfall SM estimates, with only 57% of wetting events captured by SMOS over Manitoba (Table 2). For both wetting and drying, a nonparametric Kruskal–Wallis test indicates a highly significant ($P < 0.05$) difference between the medians of all satellite products

and the in situ data. However, for drying events we note slightly better agreement with in situ data for the SMOS products (IC and L3) than the ESA CCI products (Figure 5b), with a higher proportion of anomalies of the correct sign (Table 2) and the median SM' closer to in situ (Table 3). A post-hoc Wilcoxon rank sum test reveals that while the satellite products are generally statistically significantly ($P < 0.05$) different from in situ for most cases, the distribution of anomalies from IC and in situ are not significantly different for drying over Ontario, and that at least one SMOS product is statistically significantly ($P < 0.05$) different from the ESA CCI products for most cases. This suggests that IC is the best-performing product for this metric.

Table 2. Proportion of positive and negative SM anomaly values captured by each satellite product as compared to in situ networks. The highest ratio values for each location and for each sign of anomaly are shown in bold.

In situ	Location	CCI3	CCI4	IC	L3
SM' > 0 (Wetting)	Ontario	0.62	0.69	0.7	0.72
	Manitoba	0.6	0.61	0.57	0.58
	Alberta	0.65	0.65	0.73	0.73
SM' < 0 (Drying)	Ontario	0.74	0.79	0.86	0.85
	Manitoba	0.55	0.61	0.75	0.75
	Alberta	0.66	0.69	0.75	0.73

Table 3. Median of positive and negative SM anomaly values for in situ and satellite products at all networks. The summary of the Kruskal–Wallis test is also included and statistical differences are significant for $P < 0.05$.

Sign of Anomaly	Location	Median of SM anomaly values					Kruskal–Wallis Test (P -values)
		In Situ	CCI3	CCI4	IC	L3	
SM' > 0 (Wetting)	Ontario	0.63	0.23	0.28	0.36	0.37	<0.05
	Manitoba	0.67	0.21	0.22	0.11	0.15	<0.05
	Alberta	0.92	0.32	0.33	0.49	0.44	<0.05
SM' < 0 (Drying)	Ontario	−0.82	−0.54	−0.54	−0.75	−0.68	<0.05
	Manitoba	−0.68	−0.09	−0.26	−0.67	−0.52	<0.05
	Alberta	−0.80	−0.34	−0.42	−0.56	−0.48	<0.05

A robust feature of the distribution of SM' in the satellite products is far fewer extreme dry anomalies than extreme wet anomalies, and this is true even for the subset of events where SM' < 0 (Figure 5b). In other words, even though the mean anomaly of the satellite products is negative for days where in situ detects drying (SM' < 0), these products still capture many individual large amplitude wetting events. We speculate that this is due to an overestimation of surface wetness in the satellite products shortly after rainfall events, where the satellite measurements may represent a thinner contributing layer of soil [25]. This behavior is observed for all networks but seems particularly pronounced for Alberta since for each condition, about 6–7 times more anomaly values from 33 stations over Alberta are used as compared to the fewer Ontario and Manitoba stations.

4. Discussion and Conclusions

Two versions of the ESA CCI SM product, v3.3 (CCI3) and v4.2 (CCI4), SMOS-L3 (L3) and a more recent SMOS product known as SMOS-IC (IC), were evaluated against regional (Ontario and Manitoba) and provincial (Alberta) in situ daily SM monitoring networks over important agricultural regions of Canada. We found that SMOS products generally show higher temporal correlations with in situ

measurements as compared to ESA CCI, irrespective of the soil texture or location. However, SMOS products tend to have larger biases, RMSD and SM variability than ESA CCI but are able to better capture anomalies, even though all products capture drying better than wetting.

Overall, ESA CCI could be more appropriate than SMOS for short period studies spanning over a few days or weeks, especially at regional scales, due to the large difference in the number of observations between them. However, given their ability to capture anomalies and SM variability at regional and provincial scales, for periods during which there are sufficient observations, SMOS is more suitable for agricultural applications over Canada than ESA CCI. We also found that, overall, CCI4 and IC outperformed their counterparts in all comparisons.

Several possible reasons have been reported for the dry bias in SMOS [26,41]. First, the sampling depth for SMOS at 0–3 cm is shallower than the in situ SM measurement at 5 cm [70]. Second, it is possible that the SM measured in situ could be overestimated due to soil compaction, especially during dry periods [71]. Third, Cui et al. [41] reported that an underestimation in surface temperature could be a factor causing the dry bias in SMOS. Finally, RFIs can increase the recorded TB in SMOS and thus a dry bias in the retrieved SM [14]. Furthermore, the drier bias in IC as compared to L3 is consistent with previous literature [72] and could be due to the small constant initial value for SM in the TB cost function in IC [32]. As for ESA CCI, in case RFIs are detected in multi-frequency retrievals, retrievals at a higher frequency such as X-band are selected [35], which could explain the smaller bias as compared to SMOS, even though the bias in ESA CCI is also characteristic of the bias present in GLDAS-Noah since its dynamic range is imposed on ESA CCI [73,74].

Our results also suggest that the “median of metrics” method is more appropriate than the more common “metrics of mean SM” method for evaluating the correlation and variability of satellite products with large in situ networks (Figure 4). While the small spatial variability for Ontario shows good representativeness of all stations, the large spatial variability over Manitoba due to high soil diversity shows weak representativeness of some stations over that network and agrees with previous literature [11,25]. However, while the low correlation values over clay soils did not have a large influence on the overall correlation for Manitoba, the observed lower SM variability of these soils can influence the comparison of trends. For instance, clay soils can retain SM longer than sandy soils due to having lower SM variability [25]. Since all satellite products showed considerable drying when the stations in Manitoba showed wetting, it could mean that the observed wetting for that network is an artefact resulting from low SM variability at the clay stations.

In Section 3.1 we showed that of the SMOS products, L3 has much higher temporal variability than IC over Ontario, as compared to Manitoba and Alberta. We speculate that L3 could be influenced by the relatively higher spatial variability in land cover over Ontario, which is not present over Manitoba and Alberta; for example, the individual satellite pixels that include the Ontario stations contain large fractions (>50%) of forest, open water, and non-agricultural land [25]. The L3 retrieval algorithm takes into account pixel land use and heterogeneity while IC does not, and therefore could be impacted by the uncertainties present in the auxiliary datasets used to characterise pixel heterogeneity [32]. We believe that other methodological differences in the IC product, such as the use of a more robust TB product, and the updated L-MEB vegetation and soil parameters [32], are less likely to explain the observed differences in SM variability. The effect of changing the TB data removes outlier retrievals that were present in L3, reducing the overall number of non-missing observations in IC; however, we compare products only for days when data is available from all products. Furthermore, updated land cover parameters in IC differ from L3 only for areas of low vegetation, while for forested areas the parameters are the same in both products [32].

This study attempted a pixel-to-point comparison, which presents well-known challenges due to inconsistencies in the spatial averaging scale of satellite products versus in situ probe measurements and the treatment of pixel heterogeneity in satellite products. Future work including spatial gridded comparison between these satellite products and reanalysis products, such as the recently released fifth generation of ECMWF reanalysis, ERA5 [75], could reveal more information about the spatial

characteristics of these products and the consistency among these different products. Finally, we note that a more recent L-band product, the Soil Moisture Active and Passive (SMAP) [20], launched in 2015, has been shown to capture relative soil moisture trends well over Canada [76]. We anticipate that future work comparing IC and SMAP for a more recent period should evaluate which of these products performs best for monitoring SM variability across Canadian agricultural regions.

Author Contributions: Conceptualization, Y.O. and C.G.F.; methodology, Y.O. and C.G.F.; software, Y.O.; formal analysis, Y.O. and C.G.F.; data curation, Y.O. and C.C.; writing—original draft preparation, Y.O.; writing—review and editing, Y.O., C.G.F. and C.C.; visualization, Y.O. All authors have read and agreed to the published version of the manuscript.

Funding: This research was funded in part by a research contract with Agriculture and Agri-Food Canada.

Acknowledgments: We thank Budong Qian and Aaron Berg for their helpful comments on earlier versions of these results.

Conflicts of Interest: The authors declare no conflict of interest.

References

1. Koster, R.D. Regions of Strong Coupling Between Soil Moisture and Precipitation. *Science* **2004**, *305*, 1138–1140. [[CrossRef](#)] [[PubMed](#)]
2. Wang, A.; Lettenmaier, D.P.; Sheffield, J. Soil Moisture Drought in China, 1950–2006. *J. Clim.* **2011**, *24*, 3257–3271. [[CrossRef](#)]
3. Koster, R.D.; Mahanama, S.P.P.; Livneh, B.; Lettenmaier, D.P.; Reichle, R.H. Skill in streamflow forecasts derived from large-scale estimates of soil moisture and snow. *Nat. Geosci.* **2010**, *3*, 613–616. [[CrossRef](#)]
4. Brocca, L.; Moramarco, T.; Melone, F.; Wagner, W.; Hasenauer, S.; Hahn, S. Assimilation of Surface- and Root-Zone ASCAT Soil Moisture Products Into Rainfall–Runoff Modeling. *IEEE Trans. Geosci. Remote Sens.* **2012**, *50*, 2542–2555. [[CrossRef](#)]
5. Hollmann, R.; Merchant, C.J.; Saunders, R.; Downy, C.; Buchwitz, M.; Cazenave, A.; Chuvieco, E.; Defourny, P.; de Leeuw, G.; Forsberg, R.; et al. The ESA Climate Change Initiative: Satellite Data Records for Essential Climate Variables. *Bull. Am. Meteorol. Soc.* **2013**, *94*, 1541–1552. [[CrossRef](#)]
6. McGinn, S.M.; Shepherd, A. Impact of climate change scenarios on the agroclimate of the Canadian prairies. *Can. J. Soil Sci.* **2003**, *83*, 623–630. [[CrossRef](#)]
7. Parry, M.L. *Climate change and world agriculture*; Earthscan Publications Ltd.: London, UK, 1990.
8. Dobriyal, P.; Qureshi, A.; Badola, R.; Hussain, S.A. A review of the methods available for estimating soil moisture and its implications for water resource management. *J. Hydrol.* **2012**, *458–459*, 110–117. [[CrossRef](#)]
9. Cosh, M.; Jackson, T.J.; Bindlish, R.; Prueger, J. Watershed scale temporal and spatial stability of soil moisture and its role in validating satellite estimates. *Remote Sens. Environ.* **2004**, *92*, 427–435. [[CrossRef](#)]
10. Krajewski, W.F.; Anderson, M.C.; Eichinger, W.E.; Entekhabi, D.; Hornbuckle, B.K.; Houser, P.R.; Katul, G.G.; Kustas, W.P.; Norman, J.M.; Peters-Lidard, C.; et al. A remote sensing observatory for hydrologic sciences: A genesis for scaling to continental hydrology. *Water Resour. Res.* **2006**, *42*. [[CrossRef](#)]
11. Adams, J.R.; McNairn, H.; Berg, A.A.; Champagne, C. Evaluation of near-surface soil moisture data from an AAFC monitoring network in Manitoba, Canada: Implications for L-band satellite validation. *J. Hydrol.* **2015**, *521*, 582–592. [[CrossRef](#)]
12. Ulaby, F.T.; Moore, R.K.; Fung, A.K. *Microwave Remote Sensing: Active and Passive. Volume 2-Radar Remote Sensing and Surface Scattering and Emission Theory*; NASA: Washington, DC, USA, 1982.
13. Wagner, W.; Lemoine, G.; Borgeaud, M.; Rott, H. A study of vegetation cover effects on ERS scatterometer data. *IEEE Trans. Geosci. Remote Sens.* **1999**, *37*, 938–948. [[CrossRef](#)]
14. Oliva, R.; Daganzo, E.; Kerr, Y.H.; Mecklenburg, S.; Nieto, S.; Richaume, P.; Gruhier, C. SMOS Radio Frequency Interference Scenario: Status and Actions Taken to Improve the RFI Environment in the 1400–1427-MHz Passive Band. *IEEE Trans. Geosci. Remote Sens.* **2012**, *50*, 1427–1439. [[CrossRef](#)]
15. Parinussa, R.M.; Meesters, A.G.C.A.; Liu, Y.Y.; Dorigo, W.; Wagner, W.; de Jeu, R.A.M. Error Estimates for Near-Real-Time Satellite Soil Moisture as Derived From the Land Parameter Retrieval Model. *IEEE Geosci. Remote Sens. Lett.* **2011**, *8*, 779–783. [[CrossRef](#)]

16. Jackson, T.J. III. Measuring surface soil moisture using passive microwave remote sensing. *Hydrol. Process.* **1993**, *7*, 139–152. [[CrossRef](#)]
17. Moran, M.S.; Peters-Lidard, C.D.; Watts, J.M.; McElroy, S. Estimating soil moisture at the watershed scale with satellite-based radar and land surface models. *Can. J. Remote Sens.* **2004**, *30*, 805–826. [[CrossRef](#)]
18. Kerr, Y.H.; Waldteufel, P.; Wigneron, J.-P.; Martinuzzi, J.; Font, J.; Berger, M. Soil moisture retrieval from space: The Soil Moisture and Ocean Salinity (SMOS) mission. *IEEE Trans. Geosci. Remote Sens.* **2001**, *39*, 1729–1735. [[CrossRef](#)]
19. Kerr, Y.H.; Waldteufel, P.; Wigneron, J.-P.; Delwart, S.; Cabot, F.; Boutin, J.; Escorihuela, M.-J.; Font, J.; Reul, N.; Gruhier, C.; et al. The SMOS Mission: New Tool for Monitoring Key Elements of the Global Water Cycle. *Proc. IEEE* **2010**, *98*, 666–687. [[CrossRef](#)]
20. Entekhabi, D.; Njoku, E.G.; O'Neill, P.E.; Kellogg, K.H.; Crow, W.T.; Edelstein, W.N.; Entin, J.K.; Goodman, S.D.; Jackson, T.J.; Johnson, J.; et al. The Soil Moisture Active Passive (SMAP) Mission. *Proc. IEEE* **2010**, *98*, 704–716. [[CrossRef](#)]
21. Jackson, T.J.; Cosh, M.H.; Bindlish, R.; Starks, P.J.; Bosch, D.D.; Seyfried, M.; Goodrich, D.C.; Moran, M.S.; Du, J. Validation of Advanced Microwave Scanning Radiometer Soil Moisture Products. *IEEE Trans. Geosci. Remote Sens.* **2010**, *48*, 4256–4272. [[CrossRef](#)]
22. Chanzy, A.; Schmugge, T.J.; Calvet, J.-C.; Kerr, Y.; van Oevelen, P.; Grosjean, O.; Wang, J.R. Airborne microwave radiometry on a semi-arid area during HAPEX-Sahel. *J. Hydrol.* **1997**, *188–189*, 285–309. [[CrossRef](#)]
23. Schmugge, T.; Jackson, T.J. Mapping surface soil moisture with microwave radiometers. *Meteorol. Atmos. Phys.* **1994**, *54*, 213–223. [[CrossRef](#)]
24. Champagne, C.; Davidson, A.; Cherneski, P.; L'Heureux, J.; Hadwen, T. Monitoring Agricultural Risk in Canada Using L-Band Passive Microwave Soil Moisture from SMOS. *J. Hydrometeorol.* **2015**, *16*, 5–18. [[CrossRef](#)]
25. Champagne, C.; Rowlandson, T.; Berg, A.; Burns, T.; L'Heureux, J.; Tetlock, E.; Adams, J.R.; McNairn, H.; Toth, B.; Itenfisu, D. Satellite surface soil moisture from SMOS and Aquarius: Assessment for applications in agricultural landscapes. *Int. J. Appl. Earth Obs. Geoinf.* **2016**, *45*, 143–154. [[CrossRef](#)]
26. Al Bitar, A.; Leroux, D.; Kerr, Y.H.; Merlin, O.; Richaume, P.; Sahoo, A.; Wood, E.F. Evaluation of SMOS Soil Moisture Products Over Continental U.S. Using the SCAN/SNOTEL Network. *IEEE Trans. Geosci. Remote Sens.* **2012**, *50*, 1572–1586. [[CrossRef](#)]
27. dall'Amico, J.T.; Schlenz, F.; Loew, A.; Mauser, W. First Results of SMOS Soil Moisture Validation in the Upper Danube Catchment. *IEEE Trans. Geosci. Remote Sens.* **2012**, *50*, 1507–1516. [[CrossRef](#)]
28. Djamai, N.; Magagi, R.; Goïta, K.; Hosseini, M.; Cosh, M.H.; Berg, A.; Toth, B. Evaluation of SMOS soil moisture products over the CanEx-SM10 area. *J. Hydrol.* **2015**, *520*, 254–267. [[CrossRef](#)]
29. Jackson, T.J.; Bindlish, R.; Cosh, M.H.; Zhao, T.; Starks, P.J.; Bosch, D.D.; Seyfried, M.; Moran, M.S.; Goodrich, D.C.; Kerr, Y.H.; et al. Validation of Soil Moisture and Ocean Salinity (SMOS) Soil Moisture Over Watershed Networks in the U.S. *IEEE Trans. Geosci. Remote Sens.* **2012**, *50*, 1530–1543. [[CrossRef](#)]
30. Lacava, T.; Matgen, P.; Brocca, L.; Bittelli, M.; Pergola, N.; Moramarco, T.; Tramutoli, V. A First Assessment of the SMOS Soil Moisture Product With In Situ and Modeled Data in Italy and Luxembourg. *IEEE Trans. Geosci. Remote Sens.* **2012**, *50*, 1612–1622. [[CrossRef](#)]
31. Al Bitar, A.; Mialon, A.; Kerr, Y.H.; Cabot, F.; Richaume, P.; Jacqueline, E.; Quesney, A.; Mahmoodi, A.; Tarot, S.; Parrens, M.; et al. The global SMOS Level 3 daily soil moisture and brightness temperature maps. *Earth Syst. Sci. Data* **2017**, *9*, 293–315. [[CrossRef](#)]
32. Fernandez-Moran, R.; Al-Yaari, A.; Mialon, A.; Mahmoodi, A.; Al Bitar, A.; De Lannoy, G.; Rodriguez-Fernandez, N.; Lopez-Baeza, E.; Kerr, Y.; Wigneron, J. SMOS-IC: An Alternative SMOS Soil Moisture and Vegetation Optical Depth Product. *Remote Sens.* **2017**, *9*, 457. [[CrossRef](#)]
33. Liu, Y.Y.; Parinussa, R.M.; Dorigo, W.A.; De Jeu, R.A.M.; Wagner, W.; van Dijk, A.I.J.M.; McCabe, M.F.; Evans, J.P. Developing an improved soil moisture dataset by blending passive and active microwave satellite-based retrievals. *Hydrol. Earth Syst. Sci.* **2011**, *15*, 425–436. [[CrossRef](#)]
34. Mudryk, L.R.; Derksen, C.; Kushner, P.J.; Brown, R. Characterization of Northern Hemisphere Snow Water Equivalent Datasets, 1981–2010. *J. Clim.* **2015**, *28*, 8037–8051. [[CrossRef](#)]

35. Dorigo, W.; Wagner, W.; Albergel, C.; Albrecht, F.; Balsamo, G.; Brocca, L.; Chung, D.; Ertl, M.; Forkel, M.; Gruber, A.; et al. ESA CCI Soil Moisture for improved Earth system understanding: State-of-the art and future directions. *Remote Sens. Environ.* **2017**, *203*, 185–215. [[CrossRef](#)]
36. González-Zamora, A.; Sánchez, N.; Pablos, M.; Martínez-Fernández, J. CCI soil moisture assessment with SMOS soil moisture and in situ data under different environmental conditions and spatial scales in Spain. *Remote Sens. Environ.* **2019**, *225*, 469–482.
37. Pratola, C.; Barrett, B.; Gruber, A.; Dwyer, E. Quality assessment of the CCI ECV soil moisture product using ENVISAT ASAR wide swath data over Spain, Ireland and Finland. *Remote Sens.* **2015**, *7*, 15388–15423. [[CrossRef](#)]
38. Ikonen, J.; Vehviläinen, J.; Rautiainen, K.; Smolander, T.; Lemmetyinen, J.; Bircher, S.; Pulliainen, J. The Sodankylä in situ soil moisture observation network: An example application of ESA CCI soil moisture product evaluation. *Geosci. Instrum. Methods Data Syst.* **2016**, *5*, 95–108. [[CrossRef](#)]
39. An, R.; Zhang, L.; Wang, Z.; Quaye-Ballard, J.A.; You, J.; Shen, X.; Gao, W.; Huang, L.J.; Zhao, Y.; Ke, Z. Validation of the ESA CCI soil moisture product in China. *Int. J. Appl. Earth Obs. Geoinf.* **2016**, *48*, 28–36. [[CrossRef](#)]
40. Peng, J.; Niesel, J.; Loew, A.; Zhang, S.; Wang, J. Evaluation of satellite and reanalysis soil moisture products over southwest China using ground-based measurements. *Remote Sens.* **2015**, *7*, 15729–15747. [[CrossRef](#)]
41. Cui, C.; Xu, J.; Zeng, J.; Chen, K.S.; Bai, X.; Lu, H.; Chen, Q.; Zhao, T. Soil moisture mapping from satellites: An intercomparison of SMAP, SMOS, FY3B, AMSR2, and ESA CCI over two dense network regions at different spatial scales. *Remote Sens.* **2018**, *10*, 33. [[CrossRef](#)]
42. Zhu, L.; Wang, H.; Tong, C.; Liu, W.; Du, B. Evaluation of ESA Active, Passive and Combined Soil Moisture Products Using Upscaled Ground Measurements. *Sensors (Basel)*. **2019**, *19*, 2718. [[CrossRef](#)]
43. Champagne, C.; White, J.; Berg, A.; Belair, S.; Carrera, M. Impact of Soil Moisture Data Characteristics on the Sensitivity to Crop Yields Under Drought and Excess Moisture Conditions. *Remote Sens.* **2019**, *11*, 372. [[CrossRef](#)]
44. EODC. Algorithm Theoretical Baseline Document (ATBD) Merging Active and Passive Soil Moisture Retrievals D2.1 Version 04.2. EODC, 2018.
45. Roy, A.; Royer, A.; Derksen, C.; Brucker, L.; Langlois, A.; Mialon, A.; Kerr, Y.H. Evaluation of Spaceborne L-Band Radiometer Measurements for Terrestrial Freeze/Thaw Retrievals in Canada. *IEEE J. Sel. Top. Appl. Earth Obs. Remote Sens.* **2015**, *8*, 4442–4459. [[CrossRef](#)]
46. Kędzior, M.; Zawadzki, J. Comparative study of soil moisture estimations from SMOS satellite mission, GLDAS database, and cosmic-ray neutrons measurements at COSMOS station in Eastern Poland. *Geoderma* **2016**, *283*, 21–31. [[CrossRef](#)]
47. Peterson, A.M.; Helgason, W.D.; Ireson, A.M. Estimating field-scale root zone soil moisture using the cosmic-ray neutron probe. *Hydrol. Earth Syst. Sci.* **2016**, *20*, 1373–1385. [[CrossRef](#)]
48. ESA. *Land Cover CCI Product User Guide Version 2.0*; ESA: Paris, France, 2017.
49. AAFC. *Real-Time In-Situ Soil Monitoring for Agriculture (RISMA) Network Metadata*; Agriculture and Agri-Food Canada: Burnaby, BC, Canada, 2019.
50. Kerr, Y.H.; Waldteufel, P.; Richaume, P.; Wigneron, J.P.; Ferrazzoli, P.; Mahmoodi, A.; Al Bitar, A.; Cabot, F.; Gruhier, C.; Juglea, S.E.; et al. The SMOS Soil Moisture Retrieval Algorithm. *IEEE Trans. Geosci. Remote Sens.* **2012**, *50*, 1384–1403. [[CrossRef](#)]
51. Wigneron, J.-P.; Kerr, Y.; Waldteufel, P.; Saleh, K.; Escorihuela, M.-J.; Richaume, P.; Ferrazzoli, P.; de Rosnay, P.; Gurney, R.; Calvet, J.-C.; et al. L-band Microwave Emission of the Biosphere (L-MEB) Model: Description and calibration against experimental data sets over crop fields. *Remote Sens. Environ.* **2007**, *107*, 639–655. [[CrossRef](#)]
52. Fernandez-Moran, R.; Wigneron, J.-P.; De Lannoy, G.; Lopez-Baeza, E.; Mialon, A.; Mahmoodi, A.; Parrens, M.; Al Bitar, A.; Richaume, P.; Kerr, Y. Calibrating the effective scattering albedo in the SMOS algorithm: Some first results. In Proceedings of the 2016 IEEE International Geoscience and Remote Sensing Symposium (IGARSS), Beijing, China, 10–15 July 2016; pp. 826–829.
53. Parrens, M.; Wigneron, J.-P.; Richaume, P.; Mialon, A.; Al Bitar, A.; Fernandez-Moran, R.; Al-Yaari, A.; Kerr, Y.H. Global-scale surface roughness effects at L-band as estimated from SMOS observations. *Remote Sens. Environ.* **2016**, *181*, 122–136. [[CrossRef](#)]

54. Owe, M.; de Jeu, R.; Holmes, T. Multisensor historical climatology of satellite-derived global land surface moisture. *J. Geophys. Res.* **2008**, *113*, F01002. [[CrossRef](#)]
55. Naeimi, V.; Scipal, K.; Bartalis, Z.; Hasenauer, S.; Wagner, W. An Improved Soil Moisture Retrieval Algorithm for ERS and METOP Scatterometer Observations. *IEEE Trans. Geosci. Remote Sens.* **2009**, *47*, 1999–2013. [[CrossRef](#)]
56. Wagner, W.; Lemoine, G.; Rott, H. A Method for Estimating Soil Moisture from ERS Scatterometer and Soil Data. *Remote Sens. Environ.* **1999**, *70*, 191–207. [[CrossRef](#)]
57. Liu, Y.Y.; Dorigo, W.A.; Parinussa, R.M.; de Jeu, R.A.M.; Wagner, W.; McCabe, M.F.; Evans, J.P.; van Dijk, A.I.J.M. Trend-preserving blending of passive and active microwave soil moisture retrievals. *Remote Sens. Environ.* **2012**, *123*, 280–297. [[CrossRef](#)]
58. Wagner, W.; Dorigo, W.; de Jeu, R.; Fernandez-Prieto, D.; Benveniste, J.; Haas, E.; Ertl, M. Fusion of active and passive microwave observations to create an essential climate variable data record on soil moisture. In Proceedings of the ISPRS Annals of the Photogrammetry, Remote Sensing and Spatial Information Sciences; XXII ISPRS Congress, Melbourne, Australia, 25 August–1 September 2012; pp. 1–7.
59. Wagner, W.; Hahn, S.; Kidd, R.; Melzer, T.; Bartalis, Z.; Hasenauer, S.; Figa-Saldaña, J.; de Rosnay, P.; Jann, A.; Schneider, S.; et al. The ASCAT Soil Moisture Product: A Review of its Specifications, Validation Results, and Emerging Applications. *Meteorol. Zeitschrift* **2013**, *22*, 5–33. [[CrossRef](#)]
60. Rodell, M.; Houser, P.R.; Jambor, U.; Gottschalk, J.; Mitchell, K.; Meng, C.-J.; Arsenault, K.; Cosgrove, B.; Radakovich, J.; Bosilovich, M.; et al. The Global Land Data Assimilation System. *Bull. Am. Meteorol. Soc.* **2004**, *85*, 381–394. [[CrossRef](#)]
61. Gruber, A.; Su, C.-H.; Zwieback, S.; Crow, W.; Dorigo, W.; Wagner, W. Recent advances in (soil moisture) triple collocation analysis. *Int. J. Appl. Earth Obs. Geoinf.* **2016**, *45*, 200–211. [[CrossRef](#)]
62. Parinussa, R.M.; Holmes, T.R.H.; Wanders, N.; Dorigo, W.A.; de Jeu, R.A.M. A Preliminary Study toward Consistent Soil Moisture from AMSR2. *J. Hydrometeorol.* **2015**, *16*, 932–947. [[CrossRef](#)]
63. van der Schalie, R.; de Jeu, R.; Parinussa, R.; Rodríguez-Fernández, N.; Kerr, Y.; Al-Yaari, A.; Wigneron, J.-P.; Drusch, M. The Effect of Three Different Data Fusion Approaches on the Quality of Soil Moisture Retrievals from Multiple Passive Microwave Sensors. *Remote Sens.* **2018**, *10*, 107. [[CrossRef](#)]
64. Crow, W.T.; Koster, R.D.; Reichle, R.H.; Sharif, H.O. Relevance of time-varying and time-invariant retrieval error sources on the utility of spaceborne soil moisture products. *Geophys. Res. Lett.* **2005**, *32*, L24405. [[CrossRef](#)]
65. R-core@R-project.org, R. `kruskal.test`. Available online: <https://www.rdocumentation.org/packages/stats/versions/3.6.2/topics/kruskal.test> (accessed on 1 February 2020).
66. R-core@R-project.org, R. `wilcox.test`. Available online: <https://www.rdocumentation.org/packages/stats/versions/3.6.2/topics/wilcox.test> (accessed on 1 February 2020).
67. Al-Yaari, A.; Wigneron, J.-P.; Dorigo, W.; Colliander, A.; Pellarin, T.; Hahn, S.; Mialon, A.; Richaume, P.; Fernandez-Moran, R.; Fan, L.; et al. Assessment and inter-comparison of recently developed/reprocessed microwave satellite soil moisture products using ISMN ground-based measurements. *Remote Sens. Environ.* **2019**, *224*, 289–303. [[CrossRef](#)]
68. Qiu, J.; Gao, Q.; Wang, S.; Su, Z. Comparison of temporal trends from multiple soil moisture data sets and precipitation: The implication of irrigation on regional soil moisture trend. *Int. J. Appl. Earth Obs. Geoinf.* **2016**, *48*, 17–27. [[CrossRef](#)]
69. Taylor, K.E. Summarizing multiple aspects of model performance in a single diagram. *J. Geophys. Res. Atmos.* **2001**, *106*, 7183–7192. [[CrossRef](#)]
70. Escorihuela, M.J.; Chanzy, A.; Wigneron, J.P.; Kerr, Y.H. Effective soil moisture sampling depth of L-band radiometry: A case study. *Remote Sens. Environ.* **2010**, *114*, 995–1001. [[CrossRef](#)]
71. Miller, C.J.; Yesiller, N.; Yaldo, K.; Merayyan, S. Impact of Soil Type and Compaction Conditions on Soil Water Characteristic. *J. Geotech. Geoenvironmental Eng.* **2002**, *128*, 733–742. [[CrossRef](#)]
72. El Hajj, M.; Baghdadi, N.; Zribi, M.; Rodríguez-Fernández, N.; Wigneron, J.; Al-Yaari, A.; Al Bitar, A.; Albergel, C.; Calvet, J.-C. Evaluation of SMOS, SMAP, ASCAT and Sentinel-1 Soil Moisture Products at Sites in Southwestern France. *Remote Sens.* **2018**, *10*, 569. [[CrossRef](#)]
73. Loew, A.; Stacke, T.; Dorigo, W.; De Jeu, R.; Hagemann, S. Potential and limitations of multidecadal satellite soil moisture observations for selected climate model evaluation studies. *Hydrol. Earth Syst. Sci.* **2013**, *17*, 3523–3542. [[CrossRef](#)]

74. Dorigo, W.A.; Gruber, A.; De Jeu, R.A.M.; Wagner, W.; Stacke, T.; Loew, A.; Albergel, C.; Brocca, L.; Chung, D.; Parinussa, R.M.; et al. Evaluation of the ESA CCI soil moisture product using ground-based observations. *Remote Sens. Environ.* **2015**, *162*, 380–395. [[CrossRef](#)]
75. Hersbach, H.; Dee, D. ERA5 reanalysis is in production, ECMWF Newsletter. *Spring* **2016**, *147*, 7.
76. Champagne, C.; Zhang, Y.; Cherneski, P.; Hadwen, T. Estimating Regional Scale Hydroclimatic Risk Conditions from the Soil Moisture Active-Passive (SMAP) Satellite. *Geosciences* **2018**, *8*, 127. [[CrossRef](#)]



© 2020 by the authors. Licensee MDPI, Basel, Switzerland. This article is an open access article distributed under the terms and conditions of the Creative Commons Attribution (CC BY) license (<http://creativecommons.org/licenses/by/4.0/>).